Published in final edited form as:
Free Radic Biol Med. 2010 July 15; 49(2): . doi:10.1016/j.freeradbiomed.2010.03.023.

A novel role for caveolin-1 in regulating endothelial nitric oxide synthase activation in response to H_2O_2 and shear stress

Jing Tian, **Yali Hou**, **Qing Lu**, **Dean A. Wiseman**, **Fabio Vasconcelos Fonsesca**, **Shawn Elms**, **David J. Fulton**, and **Stephen M. Black***
Pulmonary Vascular Disease Program, Vascular Biology Center, Medical College of Georgia, Augusta, GA 30912, USA

Abstract

Previous studies have shown that acute increases in oxidative stress induced by the addition of hydrogen peroxide (H_2O_2) can increase endothelial nitric oxide synthase (eNOS) catalytic activity via an increase in the phosphorylation of eNOS at serine 1177. However, it is unclear how increased H_2O_2 affects nitric oxide (NO) signaling when endothelial cells are exposed to biomechanical forces. Thus, the purpose of this study was to evaluate the acute effects of H_2O_2 on NO signaling in the presence or absence of laminar shear stress. We found that acute sustained increases in cellular H_2O_2 levels in bovine aortic endothelial cells did not alter basal NO generation but the NO produced in response to shear stress was significantly increased. This amplification in NO signaling was found to correlate with an H_2O_2-induced increase in eNOS localized to the plasma membrane and an increase in total caveolin-1 protein levels. We further demonstrated that overexpressing caveolin-1 increased eNOS localized to the plasma membrane again without altering total eNOS protein levels. We also found that caveolin-1 overexpression increased NO generation in response to shear stress but only in the presence of H_2O_2. Conversely, depleting caveolin-1 with an siRNA decreased eNOS localized to the plasma membrane and abolished the enhanced NO generation. Finally, we found that expressing a caveolin-1 binding-site deletion mutant of eNOS in COS-7 cells decreased its plasma membrane localization and resulted in attenuated NO production in response to calcium activation. In conclusion, we have identified a new role for caveolin-1 in enhancing eNOS trafficking to the plasma membrane that seems to be involved in priming eNOS for flow-mediated activation under conditions of oxidative stress. To our knowledge, this is the first report that H_2O_2 modulates eNOS activity by altering its subcellular location and that caveolin-1 can play a stimulatory role in NO signaling.

Keywords

Oxidative stress; Protein trafficking; Gene expression; Free radicals

Endothelial nitric oxide synthase (eNOS) produces the endothelium-derived relaxing factor nitric oxide (NO) and plays important roles in maintaining normal vascular function [1–3]. Recent studies have shown that oxidative stress can have multiple effects on NO signaling. Studies have shown that adding H_2O_2 to endothelial cells (EC) rapidly activates eNOS by PI3-kinase–Akt-mediated phosphorylation of Ser1177 on eNOS [4,5]. Prolonged exposure of EC to H_2O_2 increases eNOS expression by induction of gene transcription or an increase in mRNA half-life [6,7]. Conversely, studies have also shown that H_2O_2 can decrease eNOS activity [8] and eNOS transcription through the attenuation of the activities of the

* Corresponding author. sblack@mcg.edu (S.M. Black)..

transcription factors AP-1 [9] and Sp1 [10]. These contrasting effects seem to be due to differences in antioxidant enzyme activity [9,10]. In addition, accumulating evidence indicates that the enzymatic activity of eNOS within the endothelial cell is dependent on its intracellular distribution [11,12].

It has been shown that eNOS is compartmentalized within the cell predominantly to the plasma membrane [13,14]. However, eNOS is also found in the Golgi apparatus, cytosol, cytoskeleton, and even the nucleus [15,16]. Moreover, the subcellular localization of eNOS seems to directly affect its activity. Summarizing the hierarchy of eNOS activity in the various cell compartments, based on experimental data garnered from fraction studies and live-cell imaging, Oess and co-workers suggest that eNOS is most active on the plasma membrane, is moderately active in the Golgi, has low activity in the cytosol and cytoskeleton, and is least active in the nucleus [11].

However, most of the prior studies that have investigated the role of oxidative stress on endothelial cells have done so under static culture conditions; despite the fact that in vivo, the vascular endothelium is constantly exposed to biomechanical forces such as stretch, pressure, and shear stress [17,18]. Because vascular endothelial cells are in direct contact with blood flow and are constantly exposed to shear stress [17–19], studying the effects of oxidative stress induced by H_2O_2 on NO signaling when EC are exposed to biomechanical forces, such as shear stress, would better mimic the in vivo setting and may allow more physiologically relevant insights into the events involved in regulating NO signaling. Thus, the purpose of this study was to compare the acute effects of oxidative stress (induced by increasing the cellular levels of H_2O_2) on NO signaling in the presence and absence of biomechanical forces (mimicked by the addition of laminar shear stress). Our data indicate that sustained acute effects of increased H_2O_2 lead to enhanced NO signaling only in the presence of laminar shear stress, suggesting that H_2O_2 primes eNOS for flow-mediated activation. In addition, our data indicate that the enhanced NO signaling in the presence of both H_2O_2 and shear stress is dependent on a caveolin-1-mediated increase in eNOS trafficking to the plasma membrane. Together our data suggest that oxidative stress modulates eNOS activity by altering its subcellular location and that, in addition to its well-characterized inhibitory role on NO signaling, caveolin-1 can play a stimulatory role by enhancing eNOS localization to the plasma membrane where eNOS seems to be at its most active [11].

Materials and methods

Cell culture

Primary cultures of bovine aortic endothelial cells (BAEC) were maintained in Dulbecco's modified Eagle's medium supplemented with 10% fetal calf serum (Hyclone, Logan, UT, USA), antibiotics, and antimycotics (MediaTech, Herndon, VA, USA) at 37 °C in a humidified atmosphere of 5% CO_2–95% air. Cells were used between passages 3 and 10, seeded at ~50% confluence, and utilized when fully confluent. COS-7 cells were cultured and maintained in the same constituent medium but with a higher glucose concentration (4.5 g/L glucose).

Exposure of bovine aortic endothelial cells to H_2O_2

To generate H_2O_2, BAEC were exposed to glucose oxidase (GOx; Calbiochem, San Diego, CA, USA) to a final concentration of 5 units/ml. The chemical reaction is as follows:

$$\beta-\mathrm{D}-\mathrm{glucose}+H_2O+O+O_2 \xrightarrow{\text{glucose oxidase}} \mathrm{D}-\mathrm{glucono}-\delta-\mathrm{lactone}+H_2O_2$$

The level of H_2O_2 exposure was estimated using dichlorofluorescin diacetate (DCF-DA) fluorescence. Briefly, BAEC were preincubated with DCF-DA (20 μm) for 15 min and washed with warm PBS twice, the medium was then changed, and the cells exposed or not to GOx. Changes in DCF-DA fluorescence were then measured (0, 15, 30, 45, 60 min) using a fluorescence plate reader (Fluoroskan Ascent FL; Thermo Electron Corp., Waltham, MA, USA) at excitation 485 nm and emission 538 nm. A standard curve was generated by the DCF-DA fluorescence obtained using known concentrations of H_2O_2 (Rite Aid Pharmacy, Camp Hill, PA, USA). The fluorescence readings generated in BAEC exposed to GOx were then converted to concentrations of H_2O_2 by plotting the fluorescence units to this standard curve. We also used the Amplex red peroxide assay (Molecular Probes, Invitrogen, Eugene, OR, USA) to corroborate the amount of bona fide H_2O_2 produced by GOx. Briefly, BAEC were cultured in phenol red-free medium and exposed or not to GOx for 0, 15, 30, 45, or 60 min, and the culture medium or standards (dilutions of known concentrations of H_2O_2) were incubated with Amplex red, and the fluorescence was quantified using excitation 540 nm and emission 590 nm. The fluorescence units were then converted to concentrations of H_2O_2 using the standard curve.

Shear stress

BAEC were treated or not with GOx or 50 μM H_2O_2 for the indicated times. Laminar shear stress was applied using a cone-plate viscometer that accepts six-well tissue culture plates, as described previously [4,43,44]. This method achieves laminar flow rates that represent physiological levels of laminar shear stress in the major human arteries, which is in the range of 5–20 dyn/cm^2 [20], with localized increases to 30–100 dyn/cm^2.

Detection of NO_x

NO_x levels in the cell culture media were measured using an NO-sensitive electrode with a 2-mm-diameter tip connected to an Apollo 4000 free radical analyzer (ISO-NOP; WPI, Inc., Sarasota, FL, USA) as described [21]. Briefly, the electrode was calibrated by adding serial dilutions of KNO_2 to an assay buffer (0.1 M H_2SO_4+0.1 M KI) to generate a standard curve. Molar concentrations of NO_x were estimated using the standard curve.

Plasma membrane isolation

Plasma membrane was isolated from cells using the Mem-PER Eukaryotic Membrane Protein Extraction Reagent Kit (Pierce, Rockford, IL, USA) according to the manufacturer's protocol and as we have previously described [22]. Briefly, 5×10^6 cells were pelleted by centrifugation and then lysed with Reagent A followed by incubation with (1:2) Reagents B and C. The supernatant obtained by centrifugation at 10,000×*g* for 3 min was incubated at 37 °C for 20 min to separate the membrane protein fraction. The tubes were centrifuged at 10,000 *g* for 2 min and the hydrophobic phase (bottom layer) was carefully separated from the hydrophilic phase (top layer). The hydrophobic phase contained the plasma membrane fraction. The membrane proteins were subsequently purified using the SDS–PAGE Sample Prep Kit (Pierce) to eliminate excessive detergent and the protein concentrations determined using the BCA (Pierce) method to ensure equal loading in the subsequent analyses.

Immunoprecipitation and Western blotting

BAEC were solubilized with a lysis buffer containing 1% Triton X-100, 20 mM Tris, pH 7.4, 100 mM NaCl, 1 mM EDTA, 1% sodium deoxycholate, 0.1% SDS, and protease inhibitor cocktail (Pierce). Insoluble proteins were precipitated by centrifugation at 13,000 rpm for 10 min at 4 °C, and the supernatants were then incubated overnight with an anti-caveolin-1 antibody (2 μg; BD Transduction Laboratories, San Jose, CA, USA) at 4 °C followed by incubation in protein G plus protein A–Sepharose (Calbiochem) for 2 h. The

immune complexes were precipitated by centrifugation, washed three times with lysis buffer, boiled in SDS sample buffer, and subjected to SDS–PAGE on 4–12% polyacrylamide gels and transferred to a nitrocellulose membrane (Bio-Rad, Hercules, CA, USA). The membranes were blocked with 2% BSA in Tris-buffered saline containing 0.1% Tween. Protein bands were visualized by exposing the membrane to Supersignal West Femto Maximum Sensitivity Substrate (Pierce) and quantified using a Kodak Image Station 440. The monoclonal antibodies directed against phospho-Ser1177 eNOS, phospho-Thr495 eNOS, eNOS, caveolin-1, and β-actin were obtained from BD Transduction Laboratories. The antibodies against phospho-Akt (Ser473) and Akt were from Cell Signaling (Boston, MA, USA).

Real-time RT-PCR analysis

Real-time RT-PCR was employed to evaluate changes in the levels of caveolin-1 mRNA in response to H_2O_2. Primers were designed by Primer 3. The sequences were caveolin-1 forward, 5′-AGCCCAACAA CAAGGCTATG-3′, and reverse, 5′-GATGCCATCGAAACTGTGTG-3′; β-actin forward, 5′-CTCTTCCAGCCTTCCTTCCT-3′, and reverse, 5′-GGGCAGTGATCTCTTTCTGC-3′. Real-time RT-PCR was carried out in two steps. First, total RNA was extracted from cells using the RNeasy kit (Qiagen, Valencia, CA, USA), and 1 μg of total RNA was reverse-transcribed using the QuantiTect Reverse Transcription Kit (Qiagen) in a total volume of 20 μl. Quantitative real-time PCR was conducted on an Mx4000 (Stratagene, La Jolla, CA, USA), using 2 μl of RT product, 12.5 μl of QuantiTect SYBR Green PCR Master Mix (Qiagen), and primers (400 nM) in a total volume of 25 μl. The following thermo-cycling conditions were employed: 95 °C for 10 min, followed by 95 °C for 30 s, 55 °C for 60 s, and 72 °C 30 s for 45 cycles. The threshold cycles (C_t) of a serially diluted control sample were plotted to generate a standard curve. The concentration of each sample was calculated by interpolating its C_t on the standard curve and then normalized to β-actin (housekeeping gene) mRNA levels.

Overexpression of caveolin-1

An adenoviral construct for wild-type caveolin-1 (AdWTCav) was prepared using a cDNA insert obtained from the ATCC (Manassas, VA, USA). The virus was amplified in HEK-293 cells and titered. BAEC at ~90% confluence were transduced using an approximate multiplicity of infection of 50:1. An adenovirus containing the green fluorescent protein (AdGFP) was used to control for cellular effects due to adenoviral gene transduction. After 48 h to allow for protein expression the cells were harvested for the appropriate experimental procedures.

siRNA-mediated decrease in caveolin-1 expression

BAEC grown to 70% confluence were transfected with 5 nM human Hs_Cav1_10 siRNA (validated siRNA, Cat. No. SI00299642) or scrambled siRNA (Cat. No. 1022076) using HiPerFect transfection reagents (Qiagen). Cells were harvested 48 h after transfection for the appropriate experimental procedures. Western blotting was used to confirm depletion of caveolin-1 protein levels.

Transient transfection of COS-7 cells

An eight-codon deletion in the caveolin-1 binding site was introduced into the bovine eNOS-GFP construct that has been previously described [23,24]. The deleted sequence in the open reading frame of the bovine eNOS sequence was ^{1049}GTTCTCCGCGGCCCCCTTCAGCGGCTG^{1075}, which corresponds to the amino acid sequence ^{350}FSAAPFSG^{357} in the caveolin-1 binding site of eNOS. COS-7 cells (with

minimal endogenous eNOS expression) were transiently transfected with either wild-type bovine eNOS-GFP or the eNOS-GFP with the caveolin-1 binding site deletion using Effectene transfection reagents (Qiagen). Forty-eight hours post-transfection the cells were harvested for the appropriate experimental procedures.

Plasma membrane localization of eNOS using high-resolution fluorescence microscopy

To determine the fraction of eNOS localized to the plasma membrane, COS-7 cells were transiently transfected with either wild-type bovine eNOS-GFP or the eNOS-GFP with the caveolin-1 binding site deletion. After 24 h the cells were split and reseeded onto glass coverslips for a further 24 h and then subjected to fluorescence microscopy using a DeltaVision Personal DV fluorescence microscope (Applied Precision, Issaquah, WA, USA). The plasma membrane localization of eNOS was determined by calculating green fluorescence (for eNOS-GFP) using the Image Pro Plus 5 software. The magnification used was 100×, and at least 10 fields were visualized per sample.

Statistical analysis

Statistical calculations were performed using the GraphPad Prism version 4.01 software. The mean±SD was calculated for all samples and significance determined by either the unpaired *t* test or ANOVA. For the ANOVA, Neumann–Keuls post hoc testing was also performed. A value of $P<0.05$ was considered significant.

Results

Acute exposure of bovine aortic endothelial cells to H_2O_2 potentiates the shear-stress-induced increase in NO generation

Rather than adding bolus doses of labile H_2O_2, we utilized a GOx-based system to be able to maintain a more constant level of elevated H_2O_2. Our initial data indicate that H_2O_2 levels increased immediately after the addition of GOx, reaching a plateau at 30 min (Figs. 1A and B; 60.5 μM vs 61.7 μM, respectively, $P<0.05$ vs $T=0$). This level was kept constant for at least a further 30 min (Figs. 1A and B). NO_x levels were then determined in BAEC exposed or not to GOx (30 min) followed by acute exposure to laminar shear stress (20 dyn/cm^2, 15 min). Although H_2O_2 alone did not increase NO_x levels, there was a potentiation in NO_x generation in the presence of shear stress (from 226 to 443 nM, $P<0.05$ vs shear alone), and this effect could be completely abolished by pretreatment with PEG-catalase (100 units/ml) for 30 min (Fig. 1C). In addition, we confirmed that the addition of a bolus dose of H_2O_2 (50 μM) did not significantly alter basal NO_x production, whereas it significantly increased NO_x production when added with shear stress (from 188 to 341 nM, $P<0.05$ vs shear alone, Fig. 1D). We further demonstrated that the administration of H_2O_2 (GOx 5 units/ml, Fig. 1E, or 50 μM bolus H_2O_2, Fig. 1F) after BAEC had been preexposed to shear stress (20 dyn/cm^2, 8 h) also potentiated NO_x production. This priming event is not limited to shear-mediated activation of eNOS, as a similar enhancement in NO_x generation was observed in cells exposed to GOx in combination with the calcium mobilizing agent A23187 (Fig. 2). These data suggest that modestly increased levels of H_2O_2 lead to a priming of eNOS for activation rather than directly activating the enzyme itself.

H_2O_2 increases eNOS localization to the plasma membrane

To elucidate the mechanism by which H_2O_2 primes eNOS for shear-mediated eNOS activation, we first determined if there was a redistribution of eNOS in response to H_2O_2. We found that H_2O_2 (GOx 5 units/ml or 50 μM bolus H_2O_2) significantly increased the plasma membrane localization of eNOS (Figs. 3A and B) without altering total eNOS protein levels (Figs. 3C and D). Furthermore, we found that H_2O_2 (in a pp60^{Src}-dependent

manner), but not acute shear stress alone, increased Ser1177 phosphorylation of eNOS (Fig. 3E). In addition, we found that there was a synergistic effect of both stimuli that could be attenuated, at least in part, by Src kinase inhibition (Fig. 3E). We then demonstrated that H_2O_2 alone or in combination with shear activated PI3 kinase–Akt signaling with no synergistic effect (Fig. 3F). This increase in PI3 kinase–Akt signaling resulted in an increase in eNOS phosphorylation at Ser1177 (Fig. 3F). However, the increase in Ser1177 phosphorylation was higher in the presence of GOx and shear stress compared to either treatment alone (Fig. 3F). In addition, our data indicate that the inhibition of PI3 kinase did not inhibit the phosphorylation of eNOS at Ser1177 under static conditions but did so in the presence of shear stress (Fig. 3F). We also found that the increased plasma membrane localization of eNOS correlated with a significant increase in total caveolin-1 protein levels in the H_2O_2-exposed cells (Figs. 3G and H). The increase in caveolin-1 protein levels seems to be caused by an increase in gene expression as H_2O_2 also increased caveolin-1 mRNA levels (Fig. 3I).

Altering the cellular levels of caveolin-1 modulates the plasma membrane localization of eNOS and NO signaling in response to H_2O_2 and shear stress

As caveolin-1 levels were induced in response to acute increases of H_2O_2 we next determined if there was a relationship between total caveolin-1 levels and eNOS plasma membrane localization. We found that the overexpression of caveolin-1 in BAEC using an adenoviral expression construct (Fig. 4A) had no effect on total eNOS protein levels (Fig. 4B), but led to an increase in eNOS localized to the plasma membrane (Fig. 4C). To examine the functional consequence of overexpressing caveolin-1 we determined the effect on NO_X levels in H_2O_2-exposed BAEC in the presence or absence of laminar shear stress. Under static conditions, the overexpression of caveolin-1 decreased NO_X production, regardless of H_2O_2 exposure, in agreement with the existing literature [25–27]. Similarly, under conditions of increased shear stress alone, overexpressing caveolin-1 alone did not significantly alter NO_X production compared to cells transduced with AdGFP (Fig. 4D). However, in conjunction with H_2O_2, overexpressing caveolin-1 significantly increased NO_X generation compared to the AdGFP control (Fig. 4D). To further confirm the relationship between caveolin-1 and eNOS plasma membrane localization we utilized an siRNA strategy to decrease cellular caveolin-1 protein levels in BAEC. Utilizing this approach, caveolin-1 protein levels were decreased by ~85% (Fig. 5A), again without altering total eNOS protein levels (Fig. 5B). However, decreasing caveolin-1 protein levels produced a significant decrease in eNOS localized to the plasma membrane (Fig. 5C). Functionally decreasing caveolin-1 protein levels had no effect on NO_X production under static conditions irrespective of H_2O_2 treatment (Fig. 5D), whereas under shear stress alone there was a modest inhibition of NO_X production (Fig. 5D). However, decreasing caveolin-1 protein levels significantly inhibited the priming effect of H_2O_2 on NO_X generation in response to laminar shear stress (Fig. 5D). Together these data indicate that caveolin-1 levels modulate the amount of eNOS localized to the plasma membrane and underlie the priming effect of H_2O_2 on NO signaling in response to shear stress. We further explored the effect of depleting caveolin-1 on the phosphorylation of eNOS at Ser1177 and Thr495 in the presence or absence of H_2O_2 under both static and shear conditions. We found that depleting caveolin-1 did not alter the phosphorylation of eNOS at Ser1177 under static conditions (Fig. 5E); however, it significantly inhibited the synergistic phosphorylation of eNOS at Ser1177 produced by H_2O_2 and shear (Fig. 5E). In contrast, depleting caveolin-1 decreased the phosphorylation of eNOS at Thr495 under static conditions, but increased the phosphorylation of eNOS at Thr495 in the presence of shear (Fig. 5E).

Deletion of the caveolin-1 binding site in eNOS decreases plasma membrane localization and NO signaling in response to calcium activation

To further confirm the importance of caveolin-1 in targeting eNOS to the plasma membrane, we examined the effect on plasma membrane localization of eNOS when the caveolin-1 binding site within eNOS was deleted. To accomplish this we introduced an eight-codon deletion into a bovine eNOS-GFP expression construct. We then transiently transfected COS-7 cells with either wild-type eNOS-GFP or the caveolin-1 binding-site mutant eNOS-GFP. Both constructs were equally expressed (Fig. 6A). However, there was a significant decrease in binding to caveolin-1 of the mutant eNOS protein (Fig. 6B). This correlated with a significant decrease in the amount of eNOS localized to the plasma membrane (Figs. 6C and D) and attenuated NO_x generation in response to A23187 stimulation (Fig. 6E).

Discussion

In this study, we evaluated the acute effects of oxidative stress (induced by H_2O_2 exposure) on NO signaling in the presence of the physiologically relevant stimulus laminar shear stress. We administered either sustained H_2O_2 (by giving glucose oxidase 5 units/ml) or a bolus addition of H_2O_2 (50 μM) before or simultaneous with 15 min of fluid shear stress. This meant that we were only modestly increasing H_2O_2 levels in the cell to more closely mimic a mild increase in oxidative stress that could occur biologically during, for example, periods of increased exercise [28,29]. We found that H_2O_2 did not increase NO_x production under basal conditions. However, it significantly enhanced the NO_x production in response to shear, suggesting that, rather than being a direct activator, H_2O_2 primes eNOS for activation. Further, we observed that H_2O_2 significantly increased eNOS membrane localization without altering overall eNOS expression. Because eNOS is reported to be more active on the plasma membrane [15,30], we speculated that H_2O_2-induced eNOS membrane localization is the underlying mechanism for the priming effect of eNOS activation. H_2O_2 is an important ROS in vivo, which can be constantly generated by the dismutation of superoxide spontaneously or catalyzed by superoxide dismutase [31]. H_2O_2 can also be synthesized by native enzymes such as xanthine oxidase and glucose oxidase [32]. Previous studies evaluating the regulation of eNOS by H_2O_2 have shown that H_2O_2 can activate eNOS in a variety of ways. H_2O_2 has been shown to up-regulate eNOS mRNA and protein levels upon several to 24 h of treatment [6,7]. H_2O_2 also increased the levels of phospho-Ser1177 as early as a few minutes after treatment [4,5]. Consistent with these previous findings, we did not observe significant changes in total eNOS protein levels in our acute setting of H_2O_2 treatment (less than 1 h). We did observe a significant, $pp60^{Src}$-dependent, increase in phospho-Ser1177 levels in GOx-exposed cells. Further, the Ser1177 phosphorylation was synergistically increased in combination with shear stress. Interestingly, shear alone did not increase eNOS phospho-Ser1177 levels. Therefore increases in phospho-Ser1177 levels could not solely account for increases in NO_x production, as H_2O_2 treatment alone did not increase NOx production. Keaney's group has previously shown that the direct addition of H_2O_2 to EC leads to the activation of eNOS through phosphorylation of eNOS at Ser1177 via a PI3-kinase-dependent pathway [5]. We found that the phosphorylation of Ser1177 by H_2O_2 under static conditions was dependent on a pathway other than PI3 kinase–Akt signaling, whereas the synergistic activation of Ser1177 by H_2O_2 and shear stress was PI3 kinase dependent. It has previously been shown that the MAP kinase–ERK pathway also plays an important role in H_2O_2-mediated early phosphorylation of Ser1177 under static conditions and this might account for our data [4]. Alternatively, it is possible that H_2O_2 is inhibiting oxidant-sensitive protein phosphatases, leading to enhanced phosphorylation of eNOS. We found that shear for 15 min activated Akt as measured by an increase in phosphorylation at Ser473 but did not significantly increase phospho-Ser1177 eNOS levels. As we saw a trend toward increase in Ser1177 levels, it is

likely that the Akt-mediated phosphorylation of eNOS at Ser1177 is simply lagging behind the activation of PI3 kinase–Akt and this signaling is enhanced by preexposing the cells to H_2O_2. Interestingly, the synergistic increase in Ser1177 phosphorylation by shear and H_2O_2 could be abolished by depleting caveolin-1. Depleting caveolin-1 also modifies the phosphorylation of eNOS at Thr495. As we have shown that depleting caveolin-1 can modify eNOS subcellular localization, this may have an impact on the interactions of eNOS with various kinases or phosphatases that modulate the phosphorylation of eNOS.

We found that H_2O_2 increased eNOS localized on the plasma membrane without altering total eNOS protein levels, suggesting a redistribution of eNOS in the subcellular organelles. Combining with previous findings, we suggest there are three stages of eNOS activation by H_2O_2: immediately (a few minutes), H_2O_2 activates eNOS by modifying its enzyme activity through PI3 kinase–Akt-mediated phosphorylation of Ser1177; early (30–60 min), H_2O_2 activates eNOS by modifying its subcellular localization; and late (several hours), H_2O_2 activates eNOS by increasing its mRNA and protein levels. These sequential events in the cell machinery may complement one another and ensure timely and efficient activation of eNOS to compensate for ROS-induced vascular dysfunction.

In this study we have demonstrated that H_2O_2-induced increases in caveolin-1 levels plays a positive role in eNOS activation by targeting eNOS to the plasma membrane. Caveolin-1 is the major structural protein of the plasmalemmal invagination, the caveolus, an important mobile platform for sequestering signaling molecules [33–35]. Previous studies have shown that caveolin-1 is actively involved in transporting a host of proteins to the plasma membrane. For example, dysferlin [36], the angiotensin receptor [37], the insulin receptor [38], and the stretch-activated channel short transient receptor potential channel-1 [39,40] all depend on caveolin-1 for efficient membrane delivery. Caveolin-1 also serves as a scaffold protein involved in the recruitment/association of specific signaling complexes into caveolae [34,41,42]. Caveolin-1 also interacts with a variety of signaling molecules through the caveolin scaffolding domain (CSD) [43,44]. Existing literature indicates that caveolin-1 exerts a dual mode of posttranslational regulation on eNOS activity [45–47]. On one hand, it enables the enrichment of eNOS in caveolae and compartmentalizes the enzyme for optimal activation (compartmentation effect) [13,48], whereas on the other hand, direct interaction between caveolin-1 and eNOS holds the enzyme in its inactivated state (clamp effect) [25–27]. Thus, alterations in caveolin-1 abundance or subcellular location may lead endothelial cells to favor one mode of regulation over the other and thereby alter the subtle equilibrium that governs NO generation. Our data support this conclusion because we found that modest elevations in H_2O_2 induce a “physiological level” increase in caveolin-1 that produces a “compartmentation” effect on eNOS by increasing the enzyme localized to the plasma membrane and leading to enhanced NO production in response to shear stress. However, when we overexpress caveolin-1 beyond a physiological level using an adenoviral construct the clamp effect becomes predominant, at least under static conditions. In response to shear stress we found that the clamp effect of caveolin-1 could be overcome, indicating that NO production in cells with modified caveolin-1 levels in response to shear will be the net effect of both compartmentation and clamp effects. Our findings are consistent with previous studies that demonstrate that transfection of $Cav^{-/-}$ endothelial cells with limited amounts of caveolin-1-encoding plasmids redirects the VEGFR-2 into caveolar membranes and restores the VEGF-induced eNOS activation. However, beyond a physiologic level of caveolin-1 expression, inhibitory effects on eNOS activity are observed [45,49]. In addition to showing that caveolin-1 levels modulate the amount of eNOS localized on the plasma membrane; we further demonstrated that disruption of caveolin-1–eNOS binding redirected eNOS away from the plasma membrane. This extends previous studies that have concluded that caveolin-1–eNOS interactions are only capable of inhibiting eNOS [25–27,50]. Our data convincingly show that the caveolin-1–eNOS interaction is required for targeting eNOS to

the plasma membrane and can play a positive role in eNOS activation, suggesting that the compartmentation and clamp effects of caveolin-1 on eNOS are interrelated and cannot be arbitrarily separated.

Because caveolin-1 is necessary for the biogenesis of caveolae and the latter are actively involved in dynamic vesicular trafficking [51], caveolin-1 may be involved, at least in part, in delivering eNOS to the plasma membrane. Support for this conclusion comes from studies indicating that AT_1R can bind caveolin-1 via the CSD and this is necessary for AT_1R trafficking to the caveolae [39,52], whereas disrupting the caveolus by depleting its cholesterol content also decreases eNOS on the plasma membrane [53,54]. Caveolin-1 seems to cycle from the cytosol to the endoplasmic reticulum (ER) to the Golgi complex to the plasma membrane to the cytosol [55,56]. Thus, it undergoes a recycling process similar to that of eNOS. Thus, we speculate that after eNOS enters the ER through its myristoylation site [15,16] it becomes bound to caveolin-1 and then this complex is trafficked to the caveolus on the plasma membrane. This is supported by in vivo studies that demonstrated a decrease in plasma membrane localization of both eNOS and caveolin-1 in the diabetic kidney, correlating with decreased NO bioavailability [57]. However, it is possible that the differential effects of caveolin-1 (compartmentation vs clamp effect) on eNOS are actually mediated through different pools of caveolin-1. Future studies using specific labeling of caveolin-1, eNOS, and caveolae and live-cell imaging could help to address this possibility.

We demonstrated that the levels of eNOS on the plasma membrane correlate with the amount of NO generated in response to shear stress. Shear stress is one of the most potent and physiologically important regulators of eNOS activity [18]. Our data indicate that the subcellular localization of eNOS is a novel mechanism regulating the response of eNOS to shear stress. This potentially brings a new perspective to our understanding of shear-induced NO production in vivo. Our data indicate that caveolin-1 plays a positive role in shear-induced eNOS activation by targeting eNOS to the plasma membrane. Caveolae and caveolin-1 have long been recognized as mechanosensors of shear forces [58,59]. Chronic exposure to shear stress has been shown to increase plasma membrane levels of caveolin-1 due to the redistribution of caveolin-1 from the Golgi complex to the plasma membrane leading to increased surface density of caveolae [60,61]. These changes are accompanied by increased mechanosensitivity and activation of specific signaling pathways including eNOS [60,61]. Conversely, the coupling of the flow stimulus to activate eNOS is lost in the absence of caveolin-1 and caveolae [58,59]. These previous studies all proposed that caveolin-1 and caveolae-mediated sensing of shear stress is “caveolae” dependent. We have illuminated that the enrichment of eNOS in the plasma membrane sensitizes the enzyme to shear stress, and we propose that this caveolin-1-mediated process may not necessarily be caveolae dependent, or at least not directly caveolae dependent, but rather caveolin-1 dependent because of the requirement for caveolin-1 to help traffic eNOS to the plasma membrane.

In conclusion we have shown that H_2O_2 primes eNOS for shear-induced activation via caveolin-1-mediated eNOS plasma membrane localization. To our knowledge, this is the first report that has shed light on the regulatory effects of H_2O_2 on eNOS by focusing on eNOS subcellular localization and eNOS–caveolin-1 interactions. Further, we have shown that caveolin-1 plays a positive role in H_2O_2-mediated eNOS activation under shear stress. Because vascular endothelial cells are in direct contact with blood flow and are constantly exposed to shear stress [17–19], our data have direct physiologic importance in linking mild increases in oxidative stress with enhanced NO signaling. Further, our studies complement the current knowledge on oxidative stress-mediated endothelial dysfunction by identifying

protein traf-ficking as a new regulatory mechanism by which eNOS can be positively regulated in response to oxidative stress.

Acknowledgments

This research was supported in part by Grants HL60190 (S.M.B.), HL67841 (S.M.B.), HL084739 (S.M.B.), HD057406 (S.M.B.), and R01HL085827 (D.F.), all from the National Institutes of Health, and by a grant from the Fondation LeDucq (S.M.B.). Dean Wiseman was supported in part by F32HL090198. Fabio Vasconcelos Fonseca was supported in part by NIH Training Grant 5T32HL06699.

References

1. Arnal JF, Dinh-Xuan AT, Pueyo M, Darblade B, Rami J. Endothelium-derived nitric oxide and vascular physiology and pathology. Cell. Mol. Life Sci. 1999; 55:1078–1087. [PubMed: 10442089]
2. Ignarro LJ, Buga GM, Wood KS, Byrns RE, Chaudhuri G. Endothelium-derived relaxing factor produced and released from artery and vein is nitric oxide. Proc. Natl. Acad. Sci. U. S. A. 1987; 84:9265–9269. [PubMed: 2827174]
3. Palmer RM, Ferrige AG, Moncada S. Nitric oxide release accounts for the biological activity of endothelium-derived relaxing factor. Nature. 1987; 327:524–526. [PubMed: 3495737]
4. Cai H, Li Z, Davis ME, Kanner W, Harrison DG, Dudley SC Jr. Akt-dependent phosphorylation of serine 1179 and mitogen-activated protein kinase kinase/extracellular signal-regulated kinase 1/2 cooperatively mediate activation of the endothelial nitric-oxide synthase by hydrogen peroxide. Mol. Pharmacol. 2003; 63:325–331. [PubMed: 12527803]
5. Thomas SR, Chen K, Keaney JF Jr. Hydrogen peroxide activates endothelial nitric-oxide synthase through coordinated phosphorylation and dephosphorylation via a phosphoinositide 3-kinase-dependent signaling pathway. J. Biol. Chem. 2002; 277:6017–6024. [PubMed: 11744698]
6. Drummond GR, Cai H, Davis ME, Ramasamy S, Harrison DG. Transcriptional and posttranscriptional regulation of endothelial nitric oxide synthase expression by hydrogen peroxide. Circ. Res. 2000; 86:347–354. [PubMed: 10679488]
7. Cai H, Davis ME, Drummond GR, Harrison DG. Induction of endothelial NO synthase by hydrogen peroxide via a Ca^{2+}/calmodulin-dependent protein kinase II/janus kinase 2-dependent pathway. Arterioscler. Thromb. Vasc. Biol. 2001; 21:1571–1576. [PubMed: 11597928]
8. Wedgwood S, Black SM. Endothelin-1 decreases endothelial NOS expression and activity through ETA receptor-mediated generation of hydrogen peroxide. Am. J. Physiol. Lung Cell. Mol. Physiol. 2005; 288:L480–L487. [PubMed: 15531748]
9. Kumar S, Sun X, Wedgwood S, Black SM. Hydrogen peroxide decreases endothelial nitric oxide synthase promoter activity through the inhibition of AP-1 activity. Am. J. Physiol. Lung Cell. Mol. Physiol. 2008; 295:L370–L377. [PubMed: 18556800]
10. Kumar S, Sun X, Wiseman DA, Tian J, Umapathy NS, Verin AD, Black SM. Hydrogen peroxide decreases endothelial nitric oxide synthase promoter activity through the inhibition of Sp1 activity. DNA Cell Biol. 2009; 28:119–129. [PubMed: 19105596]
11. Oess S, Icking A, Fulton D, Govers R, Muller-Esterl W. Subcellular targeting and trafficking of nitric oxide synthases. Biochem. J. 2006; 396:401–409. [PubMed: 16722822]
12. Shaul PW. Regulation of endothelial nitric oxide synthase: location, location, location. Annu. Rev. Physiol. 2002; 64:749–774. [PubMed: 11826287]
13. Garcia-Cardena G, Oh P, Liu J, Schnitzer JE, Sessa WC. Targeting of nitric oxide synthase to endothelial cell caveolae via palmitoylation: implications for nitric oxide signaling. Proc. Natl. Acad. Sci. U. S. A. 1996; 93:6448–6453. [PubMed: 8692835]
14. Robinson LJ, Michel T. Mutagenesis of palmitoylation sites in endothelial nitric oxide synthase identifies a novel motif for dual acylation and subcellular targeting. Proc. Natl. Acad. Sci. U. S. A. 1995; 92:11776–11780. [PubMed: 8524847]
15. Sakoda T, Hirata K, Kuroda R, Miki N, Suematsu M, Kawashima S, Yokoyama M. Myristoylation of endothelial cell nitric oxide synthase is important for extracellular release of nitric oxide. Mol. Cell. Biochem. 1995; 152:143–148. [PubMed: 8751160]

16. Sessa WC, Barber CM, Lynch KR. Mutation of N-myristoylation site converts endothelial cell nitric oxide synthase from a membrane to a cytosolic protein. Circ. Res. 1993; 72:921–924. [PubMed: 7680289]
17. Davies PF. Flow-mediated endothelial mechanotransduction. Physiol. Rev. 1995; 75:519–560. [PubMed: 7624393]
18. Gimbrone MA Jr. Topper JN, Nagel T, Anderson KR, Garcia-Cardena G. Endothelial dysfunction, hemodynamic forces, and atherogenesis. Ann. N. Y. Acad. Sci. 2000; 902:230–239. discussion 239-240. [PubMed: 10865843]
19. Boo YC, Jo H. Flow-dependent regulation of endothelial nitric oxide synthase: role of protein kinases. Am. J. Physiol. Cell Physiol. 2003; 285:C499–C508. [PubMed: 12900384]
20. Lin MC, Almus-Jacobs F, Chen HH, Parry GC, Mackman N, Shyy JY, Chien S. Shear stress induction of the tissue factor gene. J. Clin. Invest. 1997; 99:737–744. [PubMed: 9045878]
21. Sud N, Sharma S, Wiseman DA, Harmon C, Kumar S, Venema RC, Fineman JR, Black SM. Nitric oxide and superoxide generation from endothelial NOS: modulation by HSP90. Am. J. Physiol. Lung Cell. Mol. Physiol. 2007; 293:L1444–L1453. [PubMed: 17827253]
22. Sud N, Wells SM, Sharma S, Wiseman DA, Wilham J, Black SM. Asymmetric dimethylarginine inhibits HSP90 activity in pulmonary arterial endothelial cells: role of mitochondrial dysfunction. Am. J. Physiol. Cell Physiol. 2008; 294:C1407–C1418. [PubMed: 18385287]
23. Garcia-Cardena G, Martasek P, Masters BS, Skidd PM, Couet J, Li S, Lisanti MP, Sessa WC. Dissecting the interaction between nitric oxide synthase (NOS) and caveolin: functional significance of the NOS caveolin binding domain in vivo. J. Biol. Chem. 1997; 272:25437–25440. [PubMed: 9325253]
24. Govers R, Rabelink TJ. Cellular regulation of endothelial nitric oxide synthase. Am. J. Physiol. Renal Physiol. 2001; 280:F193–F206. [PubMed: 11208594]
25. Garcia-Cardena G, Fan R, Stern DF, Liu J, Sessa WC. Endothelial nitric oxide synthase is regulated by tyrosine phosphorylation and interacts with caveolin-1. J. Biol. Chem. 1996; 271:27237–27240. [PubMed: 8910295]
26. Michel JB, Feron O, Sacks D, Michel T. Reciprocal regulation of endothelial nitric-oxide synthase by Ca^{2+}-calmodulin and caveolin. J. Biol. Chem. 1997; 272:15583–15586. [PubMed: 9188442]
27. Feron O, Saldana F, Michel JB, Michel T. The endothelial nitric-oxide synthase–caveolin regulatory cycle. J. Biol. Chem. 1998; 273:3125–3128. [PubMed: 9452418]
28. Powers SK, Jackson MJ. Exercise-induced oxidative stress: cellular mechanisms and impact on muscle force production. Physiol. Rev. 2008; 88:1243–1276. [PubMed: 18923182]
29. Leung FP, Yung LM, Laher I, Yao X, Chen ZY, Huang Y. Exercise, vascular wall and cardiovascular diseases: an update (Part 1). Sports Med. 2008; 38:1009–1024. [PubMed: 19026018]
30. Govers R, Bevers L, de Bree P, Rabelink TJ. Endothelial nitric oxide synthase activity is linked to its presence at cell–cell contacts. Biochem. J. 2002; 361:193–201. [PubMed: 11772391]
31. Li JM, Shah AM. Endothelial cell superoxide generation: regulation and relevance for cardiovascular pathophysiology. Am. J. Physiol. Regul. Integr. Comp. Physiol. 2004; 287:R1014–R1030. [PubMed: 15475499]
32. Cai H. Hydrogen peroxide regulation of endothelial function: origins, mechanisms, and consequences. Cardiovasc. Res. 2005; 68:26–36. [PubMed: 16009356]
33. Glenney JR Jr. Tyrosine phosphorylation of a 22-kDa protein is correlated with transformation by Rous sarcoma virus. J. Biol. Chem. 1989; 264:20163–20166. [PubMed: 2479645]
34. Parton RG, Simons K. The multiple faces of caveolae. Nat. Rev. Mol. Cell Biol. 2007; 8:185–194. [PubMed: 17318224]
35. Williams TM, Lisanti MP. The caveolin genes: from cell biology to medicine. Ann. Med. 2004; 36:584–595. [PubMed: 15768830]
36. Hernandez-Deviez DJ, Martin S, Laval SH, Lo HP, Cooper ST, North KN, Bushby K, Parton RG. Aberrant dysferlin trafficking in cells lacking caveolin or expressing dystrophy mutants of caveolin-3. Hum. Mol. Genet. 2006; 15:129–142. [PubMed: 16319126]
37. Wyse BD, Prior IA, Qian H, Morrow IC, Nixon S, Muncke C, Kurzchalia TV, Thomas WG, Parton RG, Hancock JF. Caveolin interacts with the angiotensin II type 1 receptor during exocytic

transport but not at the plasma membrane. J. Biol. Chem. 2003; 278:23738–23746. [PubMed: 12692121]

38. Cohen AW, Razani B, Wang XB, Combs TP, Williams TM, Scherer PE, Lisanti MP. Caveolin-1-deficient mice show insulin resistance and defective insulin receptor protein expression in adipose tissue. Am. J. Physiol. Cell Physiol. 2003; 285:C222–C235. [PubMed: 12660144]
39. Brazer SC, Singh BB, Liu X, Swaim W, Ambudkar IS. Caveolin-1 contributes to assembly of store-operated Ca^{2+} influx channels by regulating plasma membrane localization of TRPC1. J. Biol. Chem. 2003; 278:27208–27215. [PubMed: 12732636]
40. Maroto R, Raso A, Wood TG, Kurosky A, Martinac B, Hamill OP. TRPC1 forms the stretch-activated cation channel in vertebrate cells. Nat. Cell Biol. 2005; 7:179–185. [PubMed: 15665854]
41. Minshall RD, Sessa WC, Stan RV, Anderson RG, Malik AB. Caveolin regulation of endothelial function. Am. J. Physiol. Lung Cell Mol. Physiol. 2003; 285:L1179–L1183. [PubMed: 14604847]
42. Anderson RG. Caveolae: where incoming and outgoing messengers meet. Proc. Natl. Acad. Sci. U. S. A. 1993; 90:10909–10913. [PubMed: 8248193]
43. Li S, Couet J, Lisanti MP. Src tyrosine kinases, Galpha subunits, and H-Ras share a common membrane-anchored scaffolding protein, caveolin: caveolin binding negatively regulates the auto-activation of Src tyrosine kinases. J. Biol. Chem. 1996; 271:29182–29190. [PubMed: 8910575]
44. Couet J, Li S, Okamoto T, Ikezu T, Lisanti MP. Identification of peptide and protein ligands for the caveolin-scaffolding domain: implications for the interaction of caveolin with caveolae-associated proteins. J. Biol. Chem. 1997; 272:6525–6533. [PubMed: 9045678]
45. Sbaa E, Frerart F, Feron O. The double regulation of endothelial nitric oxide synthase by caveolae and caveolin: a paradox solved through the study of angiogenesis. Trends Cardiovasc. Med. 2005; 15:157–162. [PubMed: 16165011]
46. Feron O, Kelly RA. The caveolar paradox: suppressing, inducing, and terminating eNOS signaling. Circ. Res. 2001; 88:129–131. [PubMed: 11157661]
47. Drab M, Verkade P, Elger M, Kasper M, Lohn M, Lauterbach B, Menne J, Lindschau C, Mende F, Luft FC, Schedl A, Haller H, Kurzchalia TV. Loss of caveolae, vascular dysfunction, and pulmonary defects in caveolin-1 gene-disrupted mice. Science. 2001; 293:2449–2452. [PubMed: 11498544]
48. Shaul PW, Smart EJ, Robinson LJ, German Z, Yuhanna IS, Ying Y, Anderson RG, Michel T. Acylation targets endothelial nitric-oxide synthase to plasmalemmal caveolae. J. Biol. Chem. 1996; 271:6518–6522. [PubMed: 8626455]
49. Bauer PM, Yu J, Chen Y, Hickey R, Bernatchez PN, Looft-Wilson R, Huang Y, Giordano F, Stan RV, Sessa WC. Endothelial-specific expression of caveolin-1 impairs microvascular permeability and angiogenesis. Proc. Natl. Acad. Sci. U. S. A. 2005; 102:204–209. [PubMed: 15615855]
50. Bucci M, Gratton JP, Rudic RD, Acevedo L, Roviezzo F, Cirino G, Sessa WC. In vivo delivery of the caveolin-1 scaffolding domain inhibits nitric oxide synthesis and reduces inflammation. Nat. Med. 2000; 6:1362–1367. [PubMed: 11100121]
51. Smart EJ, Graf GA, McNiven MA, Sessa WC, Engelman JA, Scherer PE, Okamoto T, Lisanti MP. Caveolins, liquid-ordered domains, and signal transduction. Mol. Cell. Biol. 1999; 19:7289–7304. [PubMed: 10523618]
52. Ushio-Fukai M, Alexander RW. Caveolin-dependent angiotensin II type 1 receptor signaling in vascular smooth muscle. Hypertension. 2006; 48:797–803. [PubMed: 17015782]
53. Blair A, Shaul PW, Yuhanna IS, Conrad PA, Smart EJ. Oxidized low density lipoprotein displaces endothelial nitric-oxide synthase (eNOS) from plasmalemmal caveolae and impairs eNOS activation. J. Biol. Chem. 1999; 274:32512–32519. [PubMed: 10542298]
54. Xu Y, Henning RH, van der Want JJ, van Buiten A, van Gilst WH, Buikema H. Disruption of endothelial caveolae is associated with impairment of both NO^{-} as well as EDHF in acetylcholine-induced relaxation depending on their relative contribution in different vascular beds. Life Sci. 2007; 80:1678–1685. [PubMed: 17335855]
55. Monier S, Parton RG, Vogel F, Behlke J, Henske A, Kurzchalia TV. VIP21-caveolin, a membrane protein constituent of the caveolar coat, oligomerizes in vivo and in vitro. Mol. Biol. Cell. 1995; 6:911–927. [PubMed: 7579702]

56. Pol A, Martin S, Fernandez MA, Ingelmo-Torres M, Ferguson C, Enrich C, Parton RG. Cholesterol and fatty acids regulate dynamic caveolin trafficking through the Golgi complex and between the cell surface and lipid bodies. Mol. Biol. Cell. 2005; 16:2091–2105. [PubMed: 15689493]

57. Komers R, Schutzer WE, Reed JF, Lindsley JN, Oyama TT, Buck DC, Mader SL, Anderson S. Altered endothelial nitric oxide synthase targeting and conformation and caveolin-1 expression in the diabetic kidney. Diabetes. 2006; 55:1651–1659. [PubMed: 16731827]

58. Frank PG, Lisanti MP. Role of caveolin-1 in the regulation of the vascular shear stress response. J. Clin. Invest. 2006; 116:1222–1225. [PubMed: 16670766]

59. Yu J, Bergaya S, Murata T, Alp IF, Bauer MP, Lin MI, Drab M, Kurzchalia TV, Stan RV, Sessa WC. Direct evidence for the role of caveolin-1 and caveolae in mechanotransduction and remodeling of blood vessels. J. Clin. Invest. 2006; 116:1284–1291. [PubMed: 16670769]

60. Rizzo V, Morton C, DePaola N, Schnitzer JE, Davies PF. Recruitment of endothelial caveolae into mechanotransduction pathways by flow conditioning in vitro. Am. J. Physiol. Heart Circ. Physiol. 2003; 285:H1720–H1729. [PubMed: 12816751]

61. Boyd NL, Park H, Yi H, Boo YC, Sorescu GP, Sykes M, Jo H. Chronic shear induces caveolae formation and alters ERK and Akt responses in endothelial cells. Am. J. Physiol. Heart Circ. Physiol. 2003; 285:H1113–H1122. [PubMed: 12763750]

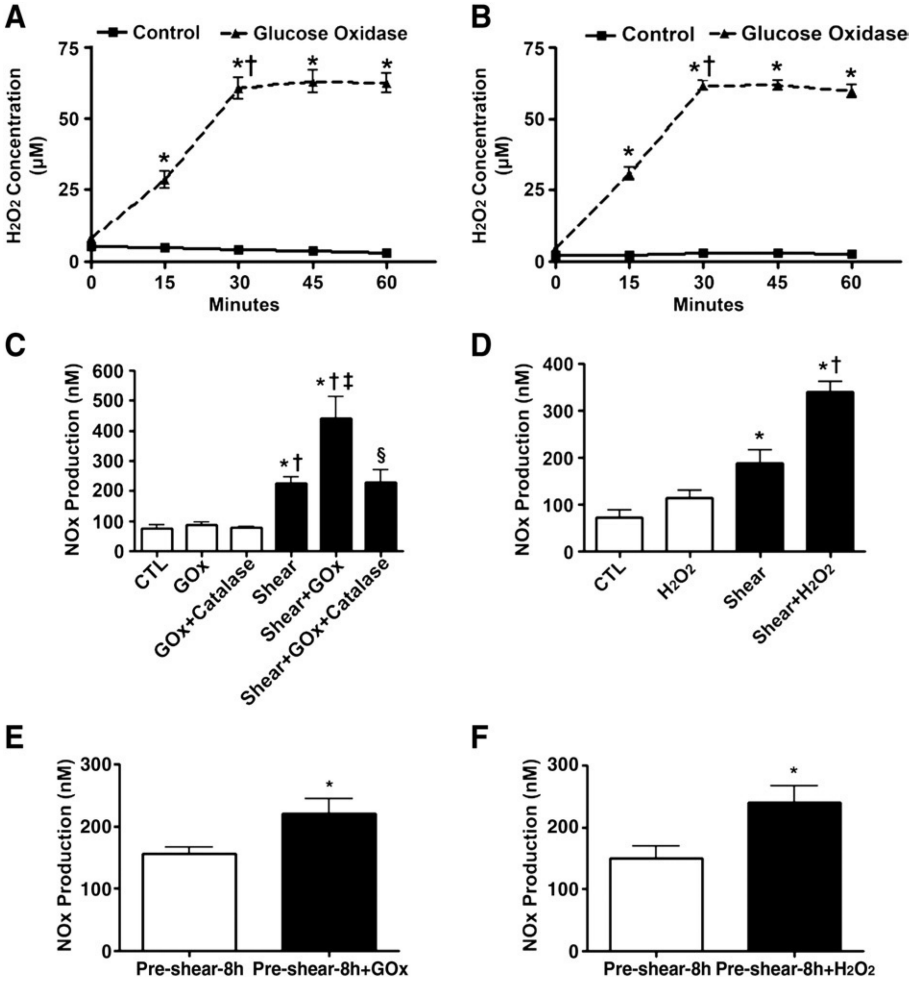

Fig. 1.

Sustained increases in H_2O_2 enhance shear-stress-mediated NO signaling in bovine aortic endothelial cells. BAEC were exposed or not to glucose oxidase (GOx, 5 units/ml) for up to 60 min. Cellular H_2O_2 levels were determined using (A) DCF-DA or (B) Amplex red fluorescence. The fluorescence readings were converted to molar concentrations of H_2O_2 by plotting the fluorescence units to a standard curve generated by DCF-DA or Amplex red staining in serially diluted known amounts of H_2O_2. H_2O_2 levels reached a plateau within 30 min and these levels were sustained through at least 60 min. Values are means±SEM; n=6; *P<0.05 vs 0 min, †P<0.05 vs previous time point. (C) BAEC were also exposed or not to H_2O_2 (GOx 5 units/ml, 30 min) in the presence or absence of PEG-catalase (100 units/ml, pretreatment for 30 min) and then acutely exposed to laminar shear stress (20 dyn/cm^2, 15 min), and NO_x levels were determined. H_2O_2 alone did not increase basal NO_x levels. However, H_2O_2 significantly potentiated shear-induced NO_x production. The enhanced NO_x generation was completely abolished by pretreatment with catalase. Values are means ±SEM; n=6; *P<0.05 vs CTL; †P<0.05 vs GOx; ‡P<0.05 vs shear alone; §P<0.05 vs shear+ GOx. (D) BAEC were also exposed or not to a bolus addition of H_2O_2 (50 μM) and then acutely exposed to laminar shear stress (20 dyn/cm^2, 15 min) and NO_x levels were determined. The addition of H_2O_2 alone did not significantly increase basal NO_x levels. However, as with GOx, the bolus addition of H_2O_2 significantly potentiated shear-induced NO_x production. Values are means±SEM; n=6; *P<0.05 vs CTL; †P<0.05 vs shear. (E and F) BAEC were also presheared (8 h, 20 dyn/cm^2), the medium was changed, and the cells

were then exposed to either GOx (5 units/ml, E) or H_2O_2 (50 μM, F) simultaneous with shear stress for a further 15 min. Both GOx and the direct addition of H_2O_2 significantly increased NO_x production compared to shear alone. Values are means±SEM; n=6; *P<0.05 vs preshear–8 h alone.

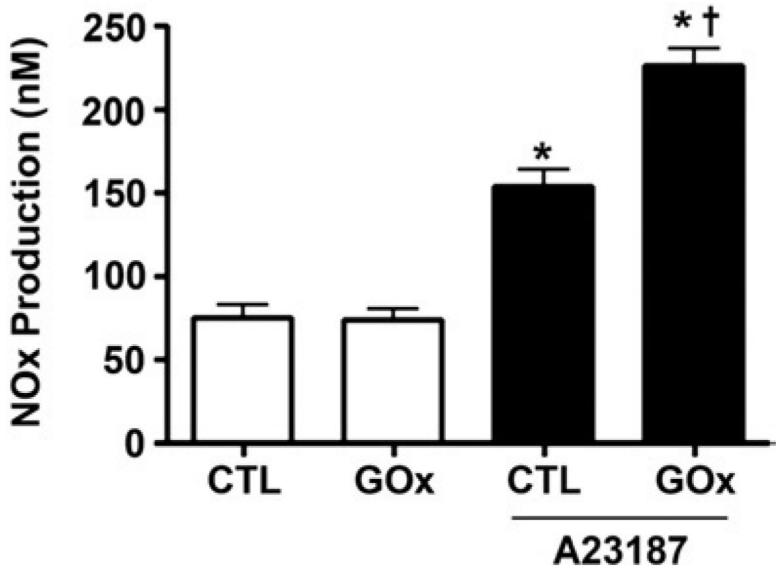

Fig. 2.

Sustained increases in H_2O_2 enhance NO generation in response to calcium stimulation in bovine aortic endothelial cells. BAEC were exposed or not to GOx (5 units/ml) for 30 min. Then the cells were treated with either vehicle (DMSO) or A23187 (2 μM) for 15 s, and NO_x levels were determined. Values are means±SEM; n=6. *P<0.05 vs no A23187; †P<0.05 vs A23187 alone.

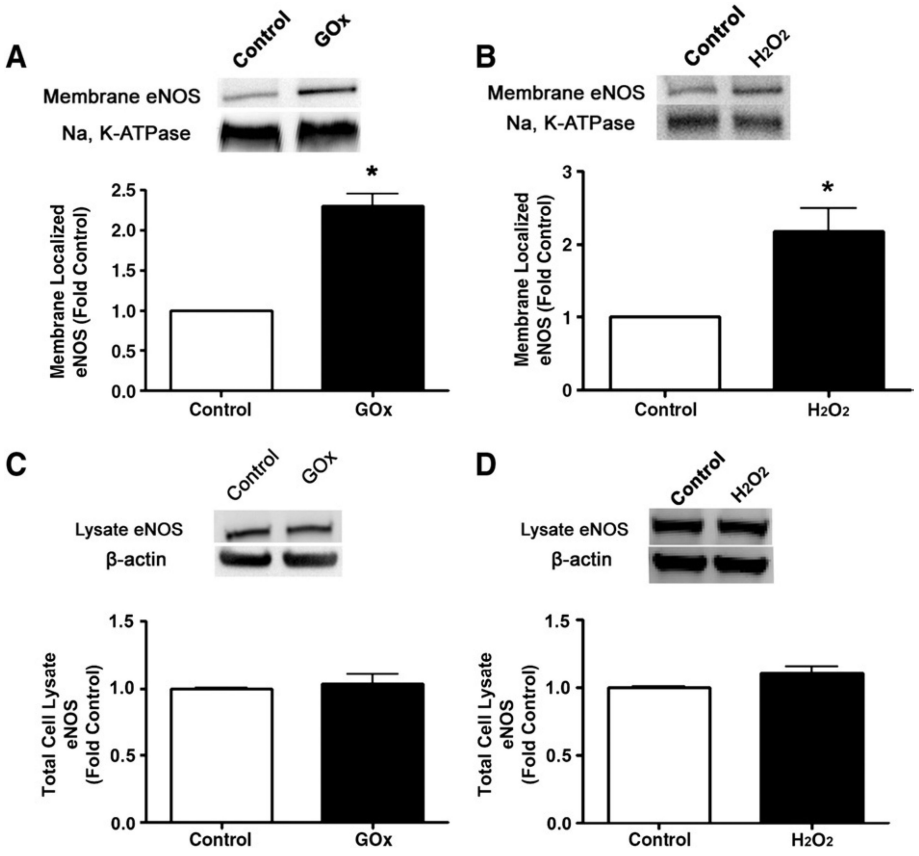

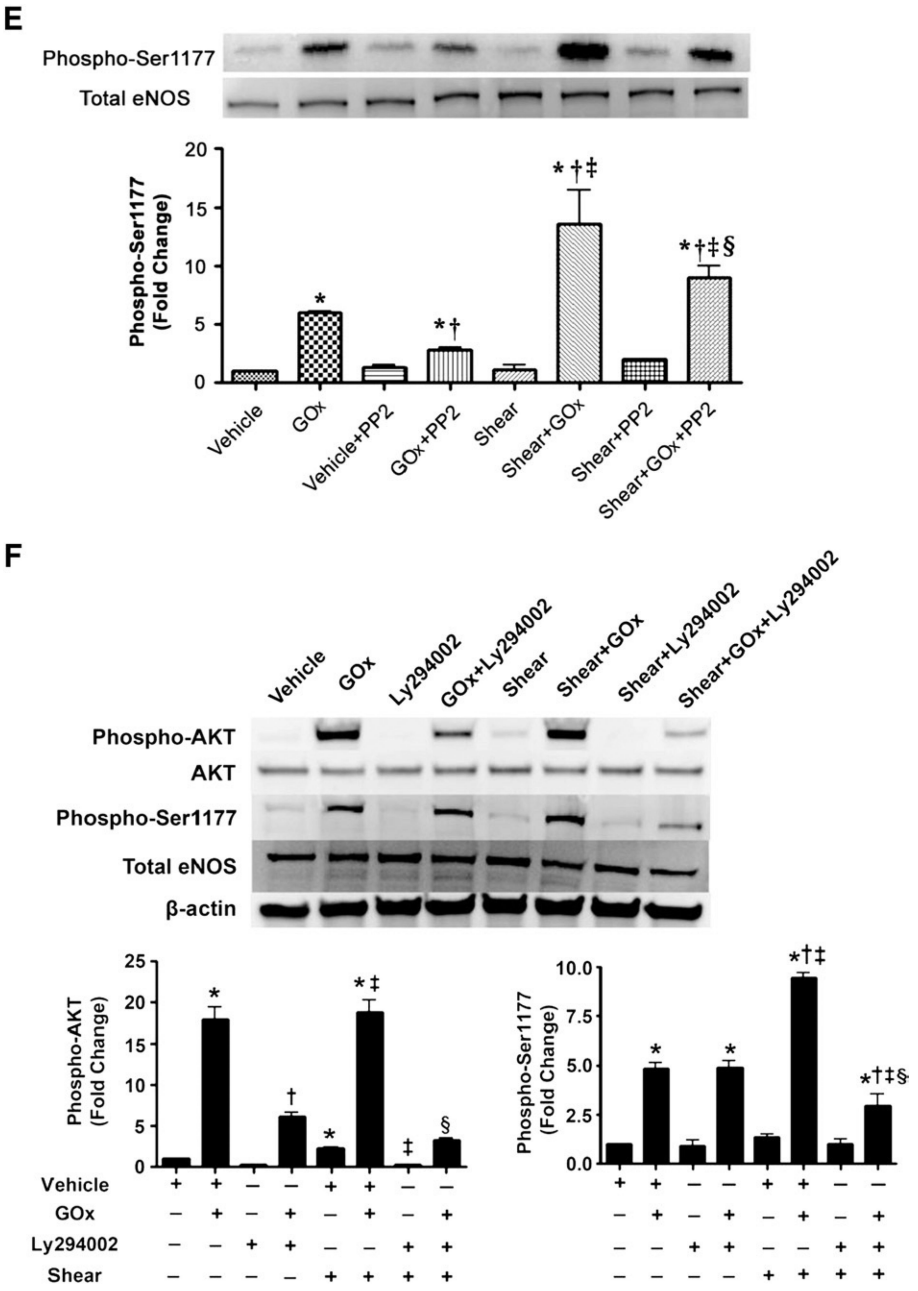

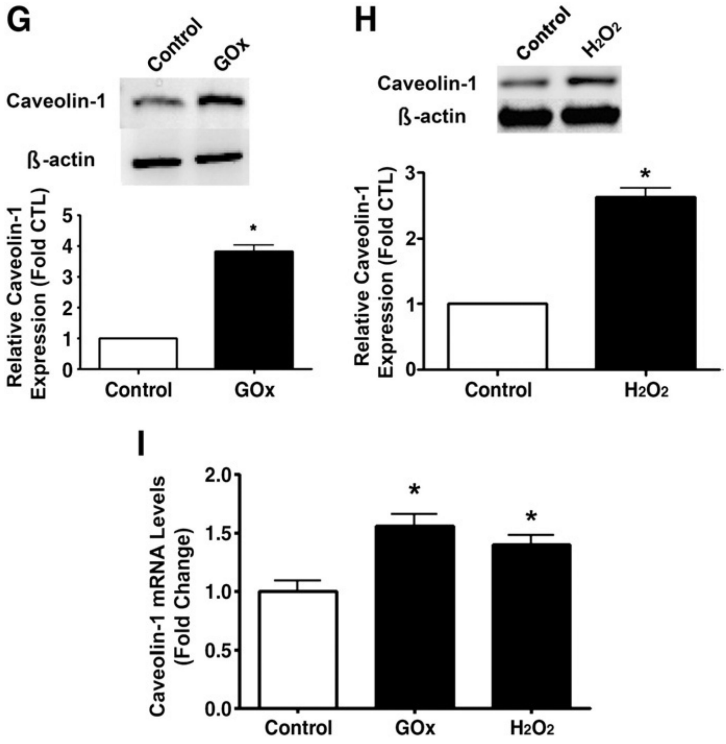

Fig. 3 (*continued*).

Fig. 3.

Acute exposure of bovine aortic endothelial cells to H_2O_2 increases eNOS localized to the plasma membrane. Confluent BAEC were exposed to H_2O_2 using (A) GOx (5 units/ml) or (B) H_2O_2 (50 μM) for 30 min and then plasma membrane fractions were prepared and membrane proteins were separated by SDS–PAGE and subjected to Western blot analysis using a specific antibody raised against eNOS. Reprobing with the membrane protein marker Na,K-ATPase was used to normalize for plasma membrane protein loading. Representative images are shown. H_2O_2 exposure significantly increased the levels of eNOS localized to the plasma membrane. In addition, total cell lysates were prepared after (C) GOx (5 units/ml) or (D) 50 μM H_2O_2 exposure, separated by SDS–PAGE, and probed with antibodies specific for eNOS. Membranes were reprobed with β-actin to normalize for loading. Representative images are shown. Acute H_2O_2 exposure did not alter total eNOS protein levels. (E) BAEC were pretreated with vehicle (DMSO) or Src kinase inhibitor, PP2 (30 μM), for 30 min, followed by incubation with GOx (5 units/ml) for 30 min, or not, and then sheared or not for 15 min. Whole-cell lysates were separated by SDS–PAGE and probed with antibodies against Ser1177 eNOS or total eNOS. Representative images are shown. Acute H_2O_2 exposure significantly increased eNOS Ser1177 phosphorylation. Further, the H_2O_2-mediated increase in Ser1177 phosphorylation was inhibited by the Src kinase inhibitor PP2. Values are means±SEM, n=3, *P<0.05 vs control; †P<0.05 vs GOx alone; ‡P<0.005 vs shear alone; §P<0.05 vs shear+GOx. (F) BAEC were pretreated with vehicle (DMSO) or the PI3 kinase inhibitor LY294002 (25 μM) for 30 min, followed by incubation or not with GOx (5 units/ml, 30 min), and then sheared or not for 15 min. Cell-lysate proteins were separated by SDS–PAGE and probed with antibodies against phospho-Akt (Ser473), Akt, phospho-Ser1177 eNOS, and total eNOS. Membranes were reprobed with β-actin to normalize for loading. Representative images are shown. The inhibition of PI3 kinase did not inhibit the phosphorylation of Ser1177 eNOS under static conditions, but significantly inhibited the phosphorylation of Ser1177 eNOS when the cells were exposed to

shear. Values are means±SEM, n=3, *P<0.05 vs vehicle; †P<0.05 vs GOx alone; ‡P<0.005 vs shear alone; §P<0.05 vs shear+GOx. Cell-lysate proteins from cells exposed or not to (G) GOx (5 units/ml, 30 min) or (H) bolus H_2O_2 (50 μM H_2O_2, 30 min) were separated by SDS–PAGE and subjected to Western blot analysis using a specific antibody against caveolin-1. H_2O_2 significantly increased caveolin-1 protein levels. (I) Total RNA was also isolated from cells exposed or not to GOx (5 units/ml, 30 min) or bolus H_2O_2 (50 μM H_2O_2, 30 min) and the levels of caveolin-1 mRNA were quantified by SYBR green real-time RT-PCR analyses. H_2O_2 significantly increased caveolin-1 mRNA levels. Data are means ±SEM, n=6, *P<0.05 vs untreated.

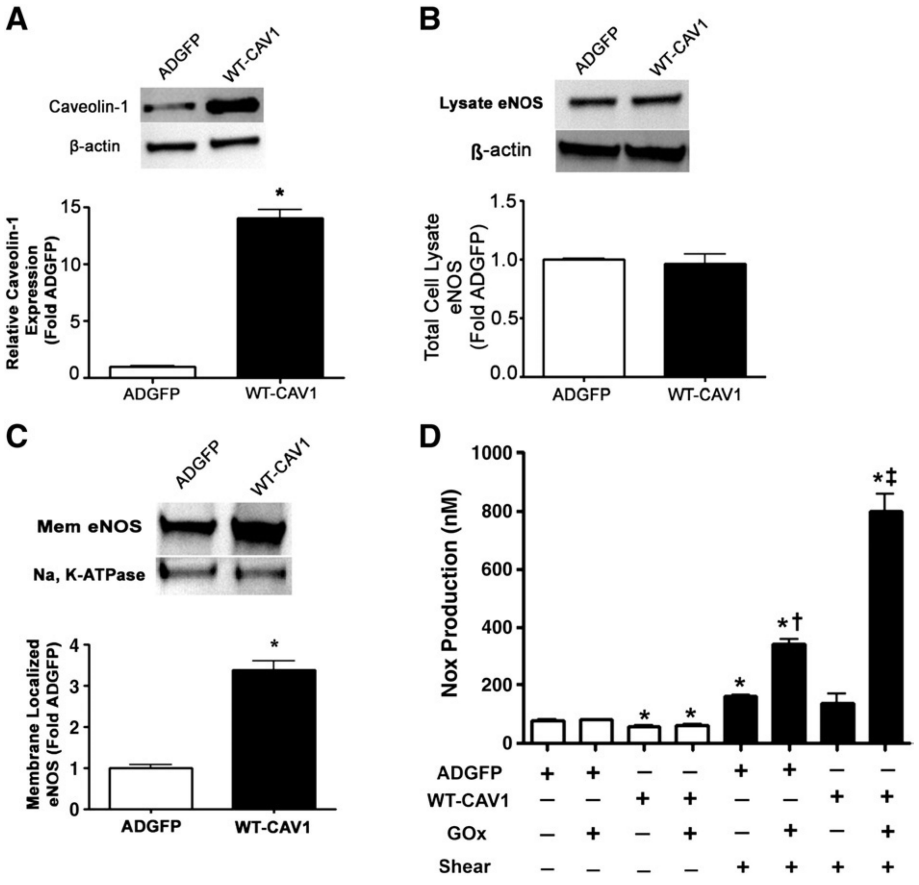

Fig. 4.

Increasing caveolin-1 protein levels stimulates eNOS plasma membrane localization and NO signaling in bovine aortic endothelial cells. BAEC were transduced with adenoviral constructs for GFP (AdGFP) or wild-type caveolin-1 (AdWTCav) at an m.o.i. of 50:1. Cells were harvested after 48 h and total lysates were separated by SDS–PAGE and probed with antibodies specific for either (A) caveolin-1 or (B) eNOS. Membranes were reprobed with β-actin to normalize for loading. Representative images are shown. Caveolin-1 was increased by ~14-fold in AdWTCav-transduced cells (A), whereas total eNOS protein levels were unchanged (B). (C) In addition, plasma membrane proteins prepared from AdGFP- and AdWTCav-transduced BAEC were separated by SDS–PAGE and subjected to Western blot analysis using a specific antibody raised against eNOS. Reprobing with the membrane protein marker Na,K-ATPase was used to normalize for plasma membrane protein loading. A representative image is shown. Caveolin-1 overexpression significantly increased the levels of eNOS localized to the plasma membrane. (D) AdGFP- or AdWTCav-transduced BAEC were also exposed or not to H_2O_2 (GOx 5 units/ml, 30 min) and then acutely exposed to laminar shear stress (20 dyn/cm^2, 15 min) and NO_x levels determined. Caveolin-1 overexpression significantly decreased NO_x levels under static conditions but NO_x levels were significantly enhanced in sheared cells in the presence of H_2O_2. Values are means ±SEM; n=3–6; *P<0.05 vs AdGFP, no shear; †P<0.05 vs ADGFP+shear; ‡p<0.05 vs WT-CAV1 + shear.

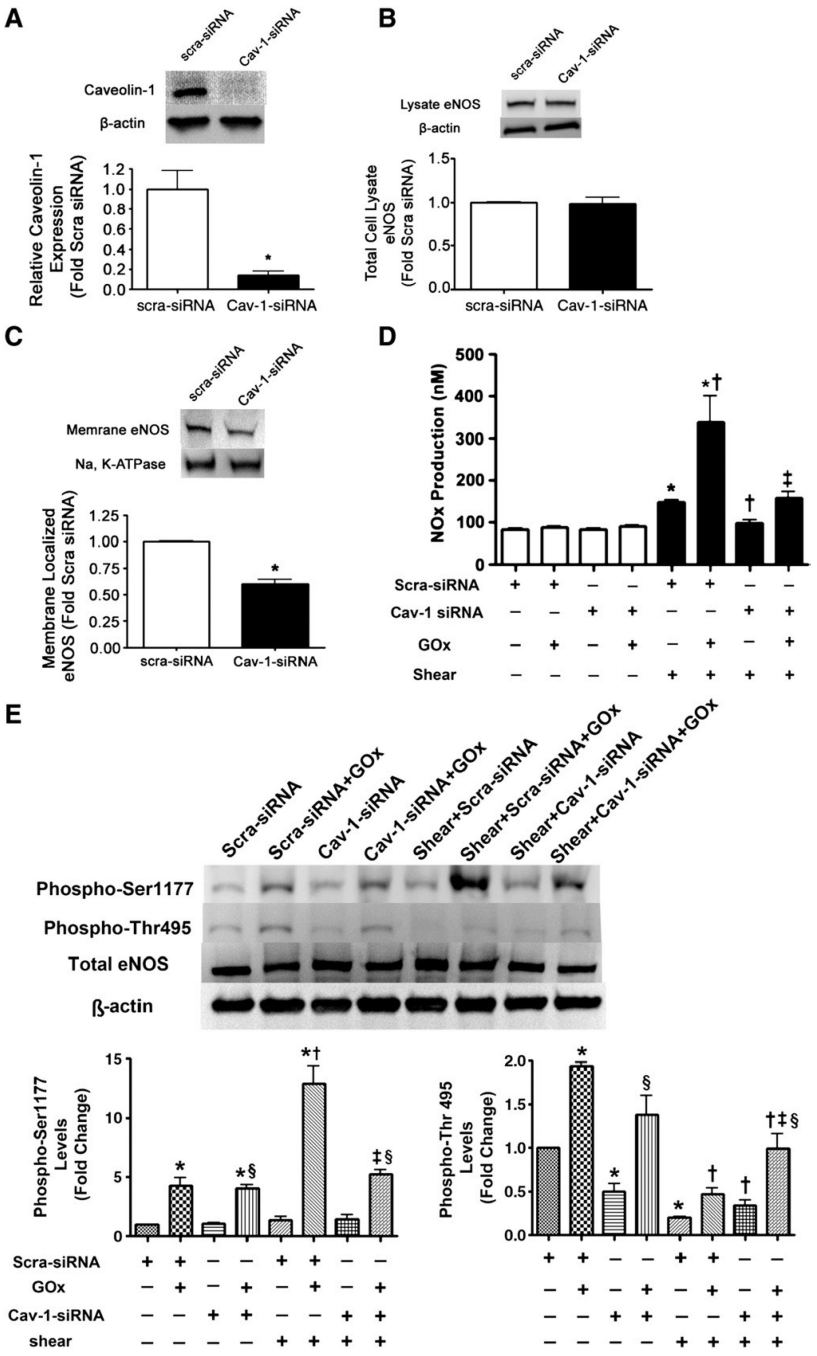

Fig. 5.

Decreasing caveolin-1 protein levels attenuates eNOS plasma membrane localization and NO signaling in bovine aortic endothelial cells. BAEC were transiently transfected with either a caveolin-1 siRNA or a scrambled siRNA (as a control). Cells were harvested after 48 h and total lysates were separated by SDS–PAGE and probed with antibodies specific for either (A) caveolin-1 or (B) eNOS. Membranes were reprobed with β-actin to normalize for loading. Representative images are shown. Caveolin-1 was decreased by ~85% in caveolin-1 siRNA-transfected cells (A), whereas total eNOS protein levels were unchanged (B). (C) In addition, plasma membrane proteins prepared from caveolin-1 siRNA- or scrambled siRNA-transfected BAEC were separated by SDS–PAGE and subjected to Western blot analysis

using a specific antibody raised against eNOS. Reprobing with the membrane protein marker, Na,K-ATPase, was used to normalize for plasma membrane protein loading. A representative image is shown. Decreasing caveolin-1 protein levels significantly decreased the levels of eNOS localized to the plasma membrane. (D) Caveolin-1 siRNA- or scrambled siRNA-transfected BAEC were also exposed or not to H_2O_2 (GOx 5 units/ml, 30 min) and then acutely exposed or not to laminar shear stress (20 dyn/cm^2, 15 min) and then NO_x levels were determined. Decreasing caveolin-1 protein levels significantly decreased NO_x levels in response to shear stress in both the presence and the absence of H_2O_2. Values are means±SEM; n=3–6; *P<0.05 vs scra-siRNA, no shear; †P<0.05 vs scra-siRNA+shear; ‡P<0.05 vs scra-siRNA+GOx+shear. (D) In addition, the effect of decreasing caveolin-1 protein levels on phospho-Ser1177 eNOS and phospho-Thr495 eNOS was determined. Decreasing caveolin-1 protein levels did not alter phospho-Ser1177 levels under static conditions but significantly inhibited the increase in phospho-Ser1177 levels in the presence of H_2O_2 and shear stress. In contrast, decreasing caveolin-1 protein levels significantly decreased phospho-Thr495 levels under static conditions while significantly increasing phospho-Thr495 levels under shear in both the absence and the presence of H_2O_2. Values are means±SEM; n=3; *P<0.05 vs scra-siRNA, no shear; †P<0.05 vs scra-siRNA+shear; ‡P<0.05 vs scra-siRNA+GOx+shear; §P<0.05, Cav-1 siRNA+GOx vs Cav-1 siRNA.

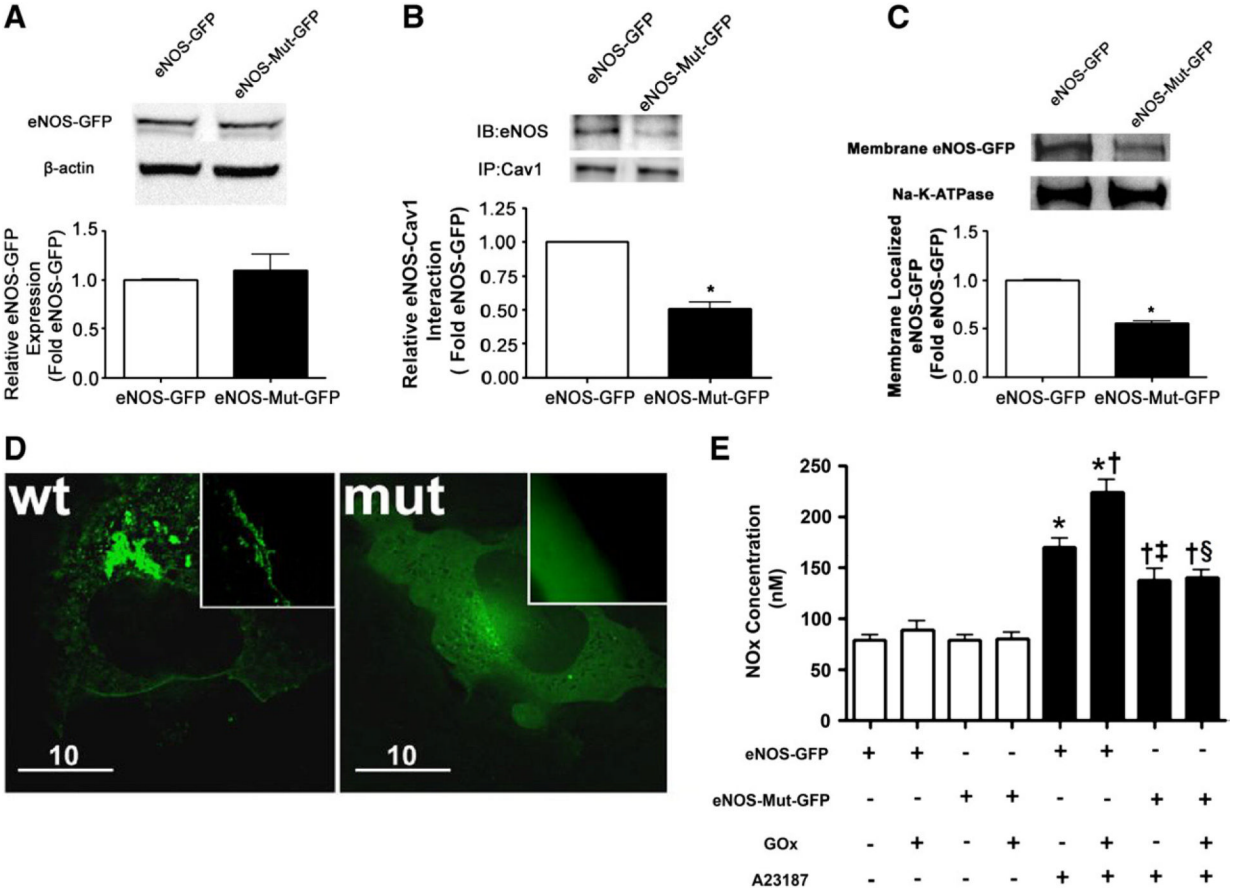

Fig. 6.

Deletion of the caveolin-1 binding site reduced the plasma membrane localization of eNOS and diminished NO generation in response to calcium stimulation. (A) COS-7 cells were transiently transfected with wild-type eNOS-GFP or the eNOS-GFP mutant with the caveolin-1 binding site deletion. After 48 h the cells were harvested and total lysates were separated by SDS–PAGE and probed with an antibody specific for eNOS. Membranes were reprobed with β-actin to normalize for loading. A representative image is shown. There is equal expression of both the wild-type and the mutant eNOS-GFP proteins. (B) Immunoprecipitation of caveolin-1 followed by Western blot analysis for eNOS using total cell extracts demonstrates that there is a decrease in eNOS–caveolin-1 interactions for the eNOS-GFP mutant with the caveolin-1 binding site deletion. Reprobing the membranes indicates that caveolin-1 levels are unchanged. A representative image is shown. (C) In addition, plasma membrane proteins prepared from COS-7 cells transiently transfected with wild-type eNOS-GFP or the eNOS-GFP mutant with the caveolin-1 binding site deletion were separated by SDS–PAGE and subjected to Western blot analysis using a specific antibody raised against eNOS. Reprobing with the membrane protein marker Na,K-ATPase was used to normalize for plasma membrane protein loading. A representative image is shown. The deletion of the caveolin-1 binding site significantly attenuated the levels of eNOS localized to the plasma membrane. Values are means±SEM, $n=3$, $^{*}P<0.05$ vs wild-type eNOS-GFP. (D) Representative fluorescence images of COS-7 cells transfected with either wild-type eNOS-GFP or the mutant eNOS-GFP with a caveolin-1 binding site deletion. Left: Wild-type eNOS-GFP displayed distinct localization on the plasma membrane. Right: Caveolin-1 binding-site-deleted eNOS-GFP showed significant decrease on the plasma membrane and exhibited an overall opaque pattern throughout the cytoplasm,

indicating the enzyme was randomly dispersed in the cytoplasm. Original magnification 100×. Each image is representative of 10 fields from three independent experiments. (E) COS-7 cells were transiently transfected with wild-type eNOS-GFP or the eNOS-GFP mutant with the caveolin-1 binding site deletion. After 48 h the cells were exposed to GOx (5 units/ml) or not for 30 min. Cells were then treated with either vehicle (DMSO) or A23187 (2 μM) and the NO_x in the culture medium was determined. The A23187-mediated increase in NO_x production was significantly attenuated in the cells expressing the eNOS-GFP mutant with the caveolin-1 binding site deletion in both the presence and the absence of GOx treatment. Wild-type eNOS-GFP also exhibited an enhanced response to A23187 stimulation after GOx treatment. Values are means±SEM; n=6–9. *P<0.05 vs no A23187; †P< 0.05 vs A23187 alone; ‡P<0.05 vs eNOS-GFP+A23187; §P<0.05 vs eNOS-GFP +A23187+GOx.